# Dynamics of solutes with hydrodynamic interactions: Comparison between Brownian dynamics and stochastic rotation dynamics simulations

G. Batôt,[1] V. Dahirel,[1] G. Mériguet,[1] A. A. Louis,[2] and M. Jardat[1,*]

[1]*UPMC Univ Paris 06, UMR CNRS 7195 PECSA, F-75005 Paris, France*

[2]*Rudolf Peierls Centre for Theoretical Physics, Department of Physics, University of Oxford, Oxford OX1 3NP, United Kingdom*

(Received 21 August 2013; published 16 October 2013)

The dynamics of particles in solution or suspension is influenced by thermal fluctuations and hydrodynamic interactions. Several mesoscale methods exist to account for these solvent-induced effects such as Brownian dynamics with hydrodynamic interactions and hybrid molecular dynamics-stochastic rotation dynamics methods. Here we compare two ways of coupling solutes to the solvent with stochastic rotation dynamics (SRD) to Brownian dynamics with and without explicit hydrodynamic interactions. In the first SRD scheme [SRD with collisional coupling (CC)] the solutes participate in the collisional step with the solvent and in the second scheme [SRD with central force coupling (CFC)] the solutes interact through direct forces with the solvent, generating slip boundary conditions. We compare the transport coefficients of neutral and charged solutes in a model system obtained by these simulation schemes. Brownian dynamics without hydrodynamic interactions is used as a reference to quantify the influence of hydrodynamics on the transport coefficients as modeled by the different methods. We show that, in the dilute range, the SRD CFC method provides results similar to those of Brownian dynamics with hydrodynamic interactions for the diffusion coefficients and for the electrical conductivity. The SRD CC scheme predicts diffusion coefficients close to those obtained by Brownian dynamic simulations without hydrodynamic interactions, but accounts for part of the influence of hydrodynamics on the electrical conductivity.

DOI: 10.1103/PhysRevE.88.043304 PACS number(s): 02.70.−c, 82.70.Dd, 66.10.C−

## I. INTRODUCTION

The numerical simulation of transport processes in ionic solutions and colloidal suspensions over time scales larger than the characteristic time of solute diffusion requires the use of simplified descriptions of the solvent. In such coarse-grained descriptions, the influence of solvent molecules on the static properties of the solutes is taken into account through effective interaction potentials averaged over the solvent degrees of freedom. Solvent molecules also influence the dynamic properties of solutes: Thermal fluctuations induce Brownian motion and momentum transfers through the solvent couple the motions of solutes. The latter effect generates the hydrodynamic interactions (HIs). Several simulation methods with coarse-grained solvent exist, which account both for the Brownian motion and for hydrodynamic interactions.

Brownian dynamics (BD), which was first proposed by Ermak and McCammon in the 1970s [1,2], can be used to investigate the dynamic properties of solutions [3–5], of colloidal suspensions [6–11], and of polymers and polyelectrolytes [12–16]. In BD, displacements of solutes are described by a stochastic equation of motion, so that the Brownian motion is explicitly accounted for, and HIs are computed due to a diffusion matrix for which approximations can be obtained in the Stokes limit. Nevertheless, the treatment of HIs in BD suffers several weaknesses: (i) Pairwise approximations of the diffusion tensor exist for bulk solutions [17], but for systems under confinement, analytic expressions of the diffusion matrix scarcely exist, except in the case of systems confined between walls [18,19]; (ii) pairwise approximations of the diffusion matrix are valid only for dilute systems, typically with volume fraction less than 10% [20]; and (iii) the BD algorithm requires the computation of the square root of the diffusion matrix at each step to generate the random displacements, a time-consuming operation.

Stochastic rotation dynamics (SRD) combined with molecular dynamics for solutes is an alternative simulation method that allows one to account for hydrodynamic couplings in any geometry and in several hydrodynamic regimes. Stochastic rotation dynamics was first introduced by Malevanets and Kapral [21] and now also goes by the name multiple-particle collision dynamics [22]. In this algorithm, the fluid is represented by pointlike particles that only interact through the so-called collision steps where momentum exchanges occur. Between collision steps, fluid particles undergo ballistic motions (in the absence of external fields). As this algorithm conserves momentum and energy, it generates the correct Navier-Stokes hydrodynamics. In order to describe solutions and suspensions, a fluid bath described via SRD can be coupled to an explicit molecular dynamics (MD) of interacting solute particles. Two different schemes exist in the literature to achieve the coupling between fluid and solutes. In the first one [22], solutes and fluid particles are treated on an equal footing: Solute particles participate in the momentum exchange during the collision step and no other interaction occurs between solutes and fluid particles. During the so-called streaming steps between collision steps, fluid particles have ballistic motions and solutes undergo standard MD moves. In the following, we will refer to this scheme as SRD with collisional coupling (CC). In the second scheme [23,24], fluid particles are coupled to solute particles through a central repulsive interaction, which excludes the fluid particles from the interior of the solutes. This interaction is taken into account within the streaming

*marie.jardat@upmc.fr

 

steps for both fluid and solute particles. Solute particles do not participate in the collision steps. In the following, we will refer to this scheme as SRD with central force coupling (CFC). These two schemes clearly do not correspond to the same hydrodynamic boundary condition between fluid and solutes. The SRD CC scheme treats the solute as a point from the hydrodynamics standpoint, which may be appropriate for polymers or small solutes, for which defining clear hydrodynamic boundaries is anyway questionable. Conversely, there is within the SRD CFC scheme a clear fluid-solute interface, on which the fluid slides. This slip boundary condition can be replaced by stick boundary conditions, at the price of algorithmic changes that make the computational cost increase [25–28] and allow the rotational diffusion of colloids to be accounted for [25]. Because of its simplicity and efficiency, the SRD CC scheme has been used in many simulations of polymers with or without external field [22,29–31] and also in simulations of colloidal suspensions [32]. The SRD CFC scheme allows, for instance, the simulation of the dynamics of colloidal suspensions in crowded conditions [33], the sedimentation of colloidal suspensions [34–36], the thermal diffusion of colloids [37], the self-assembly of colloids [27], and colloids under confinement [27,38]. The two coupling schemes (CC and CFC) have never been quantitatively compared for a given system. Only the work of Hecht *et al.* [32] suggests a qualitative agreement between both methods, but no numerical results were given in this work to quantify this agreement. Finally, it should be noted that hybrid lattice-Boltzmann–molecular dynamics simulations, which are lattice-based simulations, are another alternative to account for hydrodynamics and thermal fluctuations of the solvent in solutions and suspensions [39].

In this context, the objective of the present paper is to compare the aforementioned simulation methods (BD, SRD CC, and SRD CFC) on a simple system representative of a suspension. The question we are particularly interested in is whether these methods predict quantitatively similar dynamical properties on time scales longer than the structural relaxation time, time needed by a sphere to diffuse a distance roughly equal to its radius. An efficient simulation method that would provide reliable dynamic quantities could indeed be used to interpret experimental determinations of transport coefficients in terms of individual properties of solutes. Such a procedure based on an efficient two-scale BD scheme, for example, was recently used by some of us to deduce from experiments the size, the bare charge, and the effective charge of micelles in aqueous solutions [40,41]. However, based on BD, this procedure was limited to the case of bulk suspensions of volume fractions less than 10%. The use of SRD-based schemes would allow one to overcome this limitation.

Here we propose to compute the transport coefficients of suspensions of neutral or charged solutes for several volume fractions between 0.02 and 0.3. We compute the self-diffusion coefficient as it is useful for many applications and analytical calculations at larger scales, such as the calculation of first-passage times, residence times, or rates of diffusion-limited reactions. However, it is known that the effect of HIs on the self-diffusion coefficient is quite limited, so we also compute the electrical conductivity, a collective transport property that is more difficult to calculate but is also sensitive to hydrodynamics. Moreover, the case of charged solutes is particularly interesting because (i) most solutes in aqueous solutions (i.e., in most natural solutions) are charged, (ii) the presence of charges gives rise to important electrostatic friction effects that are significantly influenced by hydrodynamic interactions between solutes [42], and (iii) it is important to test whether the presence of attractive potentials, such as the attractive Coulomb interactions between particles of opposite charges, can lead to important deviations between the results of BD and SRD. We compare in what follows the results of BD with HIs and slip boundary conditions, SRD with collisional coupling, and SRD with central force coupling, the latter corresponding to slip solute-fluid boundary conditions. We have also computed in every case the same transport coefficients from BD simulations without HIs in order to provide a reference where the dynamics is only affected by direct interactions between solutes.

The paper is organized as follows. In Sec. II we describe the simulation methods (Brownian dynamics and SRD schemes). In Sec. III we describe the model system under study and discuss the choice of the parameters of all methods. In Sec. IV we compare the results obtained by the four algorithms concerning the structural properties, the self-diffusion coefficients of solutes, and the electrical conductivity of the charged system.

## II. SIMULATION METHODS

### A. SRD algorithms

#### 1. *Case of a pure SRD fluid*

Here we describe the SRD algorithm briefly; we use the same notations as those of Ref. [24]. The fluid in SRD is represented by pointlike particles, whose positions and velocities evolve in two steps. First, in the streaming step, positions and velocities are propagated by integrating Newton's equations of motion, for a time denoted by $\delta t_c$. In the absence of external forces, this yields a ballistic motion for each fluid particle $i$:

$$\mathbf{r}_i(t+\delta t_c) = \mathbf{r}_i(t) + \mathbf{v}_i(t)\delta t_c, \tag{1}$$

where $\mathbf{r}_i$ are $\mathbf{v}_i$ are, respectively, the position and the velocity of particle $i$. Second, in the collision step, the simulation box is divided into small cubic cells of size $a_0$, where momentum exchanges between the enclosed fluid particles occur. More precisely, a randomly oriented axis is defined for each collision cell and the velocities of fluid particles relative to the velocity of the center of mass of the cell are rotated by an angle $\alpha$ around this axis:

$$\mathbf{v}_i(t+\delta t_c) = \mathbf{v}^{\text{cell}}_{\text{c.m.}}(t) + \mathcal{R}_\alpha\left[\mathbf{v}_i(t) - \mathbf{v}^{\text{cell}}_{\text{c.m.}}(t)\right], \tag{2}$$

where $\mathcal{R}_\alpha$ is the rotation matrix and $\mathbf{v}^{\text{cell}}_{\text{c.m.}}$ the velocity of the center of mass of the cell. The angle $\alpha$ is a fixed parameter of the simulation. The collision step keeps unchanged the velocity of the center-of-mass of the cell. To ensure the Galilean invariance, a random shift of the collision grid has to be performed at each collision step [43,44].

This algorithm ensures the conservation of the local momentum of the fluid, while enabling momentum transfer inside the fluid. The SRD fluid thus has the hydrodynamic characteristics of a real fluid, in particular in terms of dimensionless hydrodynamic numbers, as discussed in more

detail in the paper of Padding and Louis [24]. The amount of momentum that is exchanged in a cell per unit time, and thus the viscosity of the SRD fluid, depends on the number of solvent particles per cell $\gamma$, on the rotation angle $\alpha$, and on the time interval between collision steps $\delta t_c$. The simplicity of the SRD algorithm makes possible the derivation of analytical formulas for the viscosity and transport coefficients as functions of $\gamma$, $\alpha$, and $\delta t_c$ [22,24]. In what follows, we use dimensionless units depending on the fluid particle mass $m_f$ as the mass unit, the size of the collision cells $a_0$ as the length unit, and $k_BT$ as the energy unit with $T$ the temperature and $k_B$ the Boltzmann constant. The time unit is then

$$t_0 = a_0\sqrt{\frac{m_f}{k_BT}}. \tag{3}$$

The value of the collision time step $\delta t_c$ controls the fluid properties by modulating the dimensionless mean free path $\lambda$ of fluid particles defined by $\lambda = \frac{\delta t_c}{t_0}$.

#### 2. *Embedded particles in a SRD bath: Collisional coupling*

The simplest method to achieve the coupling between solute particles and the fluid bath is to treat the solutes like fluid particles, except that they are interacting with each other and may have a mass different from that of fluid particles. In the streaming step, the positions of fluid particles are updated following Eq. (1), whereas the positions and velocities of solutes, denoted, respectively, by $\mathbf{R}_j$ and $\mathbf{V}_j$ for solute $j$, are propagated due to the velocity Verlet algorithm of standard MD simulations, with a time step $\delta t_{\mathrm{MD}}$:

$$\mathbf{R}_j(t+\delta t_{\mathrm{MD}}) = \mathbf{R}_j(t) + \mathbf{V}_j(t)\delta t_{\mathrm{MD}} + \frac{\mathbf{F}_j(t)}{2M}\delta t_{\mathrm{MD}}^2, \tag{4}$$

$$\mathbf{V}_j(t+\delta t_{\mathrm{MD}}) = \mathbf{V}_j(t) + \frac{\mathbf{F}_j(t)+\mathbf{F}_j(t+\delta t_{\mathrm{MD}})}{2M}\delta t_{\mathrm{MD}}, \tag{5}$$

where $M$ is the solute mass and $\mathbf{F}_j$ is the force vector acting on solute $j$ at the beginning of the step, which derives from a given interaction potential. Like in MD, the choice of $\delta t_{\mathrm{MD}}$ relies on a compromise between numerical efficiency and precision: High values enhance the efficiency but can lead to unphysical moves if the interaction force varies too much during $\delta t_{\mathrm{MD}}$. The value of the time step $\delta t_{\mathrm{MD}}$ depends then on the nature of the interaction potential and is often smaller than $\delta t_c$.

During the collision step, the velocities of every particle, in the fluid and solute, included in each collision cell are updated following Eq. (2) given above. This momentum exchange constitutes the only interaction between fluid and solute particles in this simulation scheme. Details of this simulation scheme can be found in Refs. [22,45].

#### 3. *Embedded particles in a SRD bath: Central force coupling*

In this second variant, an explicit interaction between solutes and fluid particles is introduced, which prevents fluid particles from penetrating into solutes. In contrast, solutes do not participate in the collision step. In the streaming step, both solute and fluid particles evolve according to the MD scheme of Eqs. (4) and (5). The interaction force acting on solutes contains a contribution due to other solutes and another due to fluid particles. The force acting on fluid particles is only due to solutes. Usually, the interaction potential between solutes and fluid particles is chosen to be at short range. The collision step only involves fluid particles according to Eq. (2). Details on this simulation scheme can be found in Ref. [24].

In this study, the interaction potential between fluid and embedded particles is a purely repulsive short-range Weeks-Chandler-Anderson potential

$$\phi_{\mathrm{cf}}(r) = \begin{cases} 4\epsilon_{\mathrm{cf}}\left[\left(\frac{\sigma_{\mathrm{cf}}}{r}\right)^{12} - \left(\frac{\sigma_{\mathrm{cf}}}{r}\right)^{6}\right] + \epsilon_{\mathrm{cf}} & \text{for} \quad r < 2^{1/6}\sigma_{\mathrm{cf}} \\ 0 & \text{otherwise.} \end{cases} \tag{6}$$

This interaction potential involves two parameters $\epsilon_{\mathrm{cf}}$ and $\sigma_{\mathrm{cf}}$, which must be carefully chosen as discussed in the following.

#### 4. *Comparison of the coupling schemes regarding hydrodynamic boundary conditions*

The goal of the two coupling schemes (CC and CFC) is to reproduce the momentum transferred between the fluid and the solutes. Within the CC scheme, the embedded particles are seen as point particles by the fluid particles. This is a rather crude description of local momentum exchanges, so this method should not be used when the exact description of the fluid flow field around the embedded particles needs to be resolved or when the volume or the shape of the particles is expected to influence hydrodynamic interactions. In the CFC scheme, the volume of the embedded solutes accessible to the fluid particles is clearly defined. The central force between the solutes and the fluid does not influence the tangential components of the velocities. Therefore, this coupling is analogous to hydrodynamic slip boundary conditions. Moreover, in the SRD CFC method, the position of the boundary between solute and fluid is usually chosen in such a way that it does not exactly correspond to the physical surface of the solute. Indeed, as a consequence of the representation of the solvent as particles of finite size from the point of view of solutes, a depletion interaction appears between solutes at short distances, which might not properly account for what happens in a real solvent. This issue is thoroughly discussed in Ref. [24]. To overcome this difficulty, the volume of the solute relative to the fluid particles must be smaller than the volume given by solute-solute interactions so that the fluid is allowed to flow in a small volume inside embedded solutes. For charged systems this may be a very reasonable approximation, as the solute-solute interaction range can be of considerably longer range than twice the distance that the solvent can reach from the center of the particle.

### B. Brownian dynamics algorithm

#### 1. *Brownian dynamics with hydrodynamic interactions*

Brownian dynamics is an implicit solvent simulation method based on the generalized Smoluchowski equation [46]. It is also referred to as overdamped Langevin dynamics. When HIs are taken into account, the displacements of solute particles are coupled with each other via the so-called diffusion matrix $\mathbf{D}$. This matrix depends on the position of all the particles and reflects pairwise hydrodynamic interactions. More precisely, in this simulation scheme, the equation of motion of $N$ solute particles placed in a box with periodic boundary conditions

is [1]

$$\mathbf{r}(t+\Delta t)-\mathbf{r}(t)=\left(\beta\mathbf{D}\cdot\mathbf{F}+\frac{\partial}{\partial\mathbf{r}}\cdot\mathbf{D}\right)\Delta t+\mathbf{R}, \tag{7}$$

where $\beta=1/k_BT$, $\Delta t$ is the time increment, $\mathbf{r}$ is the $3N$-dimensional configuration vector of solutes, and $\mathbf{F}$ is the interaction force acting on the particles at the beginning of the step. In addition, $\mathbf{R}$ is a random displacement, chosen from a Gaussian distribution with zero mean, $\langle\mathbf{R}\rangle=0$, and $\langle\mathbf{R}\mathbf{R}^T\rangle=2\mathbf{D}\Delta t$. Hydrodynamic interactions between particles are introduced via the configuration-dependent $3N\times 3N$ diffusion matrix $\mathbf{D}$. In this simulation scheme, the slowest operation from the computational point of view is the generation of the random displacement $\mathbf{R}$, which requires the computation of the square root of the matrix $\mathbf{D}$ at each step. In the case where hydrodynamic interactions are neglected, $\mathbf{D}$ becomes a diagonal tensor with the self-diffusion coefficient at infinite dilution of solutes on the diagonal, so the computation time is highly decreased. Compared to SRD, the treatment of hydrodynamics in BD is much less general. It is only valid in the Stokes regime and when momentum propagation is infinitely fast compared to mass propagation (infinite Schmidt number).

When the particles interact through a very steep potential, the BD algorithm can become unstable, as the random moves can drive the system into regions of high energy. This can be overcome by using a so-called Metropolized algorithm. In that case, the displacements are accepted with a given probability and unrealistic steps can be rejected. For details on this method, see [3,47–49].

To model HIs with slip boundary conditions, we use the diffusion tensor derived by Felderhof [50], assuming that HIs are pairwise additive, which is reasonable for systems with a relatively low packing fraction (smaller than 10%). The $(3N\times 3N)$ matrix $D$ can be divided into $N^2$ $(3\times 3)$ submatrices $\mathbf{D}_{ij}$:

$$\mathbf{D}=\begin{pmatrix}\mathbf{D_{11}} & \mathbf{D}_{12} & \dots & \mathbf{D}_{1N}\\ \mathbf{D}_{21} & \ddots & & \vdots\\ \vdots & & \ddots & \vdots\\ \mathbf{D}_{N1} & \dots & \dots & \mathbf{D}_{NN}\end{pmatrix}, \tag{8}$$

where

$$\mathbf{D}_{ij}(k,l)=\mathbf{D}[3(i-1)+k,3(j-1)+l] \tag{9}$$

is the element at row $k$ and column $l$ of the $(3\times 3)$ submatrix $\mathbf{D}_{ij}$.

For distinct values of $i$ and $j$, the submatrix $\mathbf{D}_{ij}$ reads

$$\mathbf{D}_{ij}=\frac{k_BT}{8\pi\eta r_{ij}^3}\left(\mathbf{I}r_{ij}^2+\mathbf{r}_{ij}\mathbf{r}_{ij}^T+4\frac{a_i^3a_j^3}{r_{ij}^6}\mathbf{r}_{ij}\mathbf{r}_{ij}^T\right) \tag{10}$$

and the submatrix $\mathbf{D}_{ii}$ is written as

$$\mathbf{D}_{ii}=D_i^0\mathbf{I}+\sum_{j=1,j\neq i}^{N}\frac{1}{6\pi\eta}\left[-\frac{3a_j^3}{2}\frac{\mathbf{r}_{ij}\mathbf{r}_{ij}^T}{r_{ij}^6}-\frac{3a_j^5}{2}\frac{\mathbf{r}_{ij}\mathbf{r}_{ij}^T}{r_{ij}^8}+\frac{3a_j^5}{16r_{ij}^6}\left(\mathbf{I}-\frac{\mathbf{r}_{ij}\mathbf{r}_{ij}^T}{r_{ij}^2}\right)\right]. \tag{11}$$

Here $D_i^\circ$ is linked to the Stokes radius by $D_i^\circ=k_BT/4\pi\eta a_i$. This expression of the diffusion tensor is a series expansion in powers of the inverse distance $1/r$ between sphere centers through the order $1/r^7$. The first two terms ($1/r^5$ and $1/r^3$) are the same as those obtained by Rotne and Prager for stick boundary conditions and for equal spheres [17]. The divergence of this matrix is not zero. We checked that neglecting the divergence of $\mathbf{D}$ in the equation of motion did not change the results of our calculations for the systems investigated here. Finally, the formulas used to compute the transport coefficients of solutes in BD are given in the Appendix.

## III. PARAMETERS OF THE SIMULATIONS

### A. Interaction potentials and length scales

We investigate the dynamic properties of solutes in prototypes of aqueous solutions or suspensions at equilibrium. The solutes are either neutral spherical particles or charged spherical ones. In the latter case, the whole system is neutral: It contains an equal number of positively and negatively charged solutes. The absolute value of the charge is $Ze$, with $e$ the elementary charge. Electrostatic interactions in such systems are known to have a great influence on the dynamic properties: They yield a strong decrease of the self-diffusion coefficient compared to the case of neutral solutes. Hydrodynamic interactions are known to increase slightly the self-diffusion coefficients and to strongly decrease the collective transport properties such as collective diffusion [51] and the electrical conductivity [3]. For the charged systems, we use here a model close to the so-called primitive model of electrolytes, with a soft short-range repulsion between solutes instead of the hard-sphere repulsion of the primitive model.

The interaction pair potential between solutes $i$ and $j$ contains in every case a short-range repulsive contribution

$$\phi_{\rm cc}(r_{ij})=4\epsilon\left(\frac{\sigma_{\rm cc}}{r_{ij}}\right)^{24}, \tag{12}$$

where $r_{ij}$ is the distance between particles $i$ and $j$ and $\sigma_{\rm cc}$ is a size parameter. The energy parameter of the short-range repulsion, $\epsilon=0.25k_BT$, is large enough to ensure that we have in every case spherical solutes of diameter $\sigma_{\rm cc}$. These interactions are computed with a minimum image convention and a cutoff distance of $2.5\sigma_{\rm cc}$.

For suspensions of neutral solutes, the short-range repulsion is the only contribution to the direct interaction between solutes. As in the case of hard spheres, there is thus only one relevant length scale in the problem, which is the particle size $\sigma_{\rm cc}$. If $\sigma_{\rm cc}$ is used as the unit length, the trajectories of the simulations are the same whatever the size of the spheres, for a given value of the volume fraction $\Phi$ of solutes, defined by $\Phi=N\pi\sigma_{\rm cc}^3/6L_{\rm box}^3$, with $L_{\rm box}$ the simulation box length and $N$ the number of solutes in the simulation box. In other words, a given simulation can describe either small solutes of nanometric size or large colloids of micrometric size.

In the case of charged solutes, the electrostatic contribution to the pair interaction potential is

$$\phi_{\rm elec}(r_{ij})=\frac{Z_iZ_je^2}{4\pi\varepsilon_0\varepsilon_r r_{ij}}=k_BTZ_iZ_j\frac{l_B}{r_{ij}}, \tag{13}$$

with $Z_i e$ the charge of particle $i$, $\varepsilon_0$ the permittivity of vacuum, $\varepsilon_r$ the relative permittivity of the solvent, and $l_B$ the Bjerrum length ($l_B = e^2/4\pi\varepsilon_0\varepsilon_r k_B T$). For suspensions of charged solutes, there are thus two different length scales $l_B$ and $\sigma_{cc}$. If $\sigma_{cc}$ is used as the unit length, for given values of $\Phi$ and of $Z_i Z_j \frac{l_B}{\sigma_{cc}}$, the trajectories obtained from simulations are the same whatever the real (physical) size of the spherical solutes. Electrostatic interactions are computed using the Ewald summation technique with conducting boundary conditions. The parameters of this summation are exactly the same in BD and in SRD calculations.

### B. Systems under study

The volume fraction $\Phi$ of systems investigated hereafter ranges between 0.019 to 0.263. In every case, we have $N = 300$ solute particles in the simulation box and we vary the density of solutes by changing the simulation box length. The charged systems contain an equal number of positively and negatively charged solutes, with $D_+^\circ = D_-^\circ$ in Brownian dynamics and with similar masses in SRD simulations. The size parameter is $\sigma_{cc}$ in every case and the hydrodynamic radius $a_i$ is equal to $\sigma_{cc}/2$. The dimensionless parameter $Z_i Z_j \frac{l_B}{\sigma_{cc}}$, which represents the electrostatic interaction at contact divided by $k_B T$, is equal to 1.785 in every case. In water at room temperature ($T = 298$ K), this value corresponds either to the case of a simple monovalent salt with ions of size equal to 0.4 nm or to the case of two nanoparticles of opposite charge (with $Z = \pm 3$) and radius of about 1 nm.

### C. Choice of parameters of the SRD simulations

One goal in this paper is to compare for the same systems the results of two different coupling schemes between solutes and a SRD bath. Both algorithms involve several parameters that control the behavior of the fluid and the coupling with solutes. The values of the mean free path $\lambda$, of the number of fluid particles in a cell $\gamma$, of the rotation angle $\alpha$, of the mass of the solute $M$, of the box length $L_{box}$, and of the interaction length $\sigma_{cf}$ in the SRD CFC scheme must be carefully chosen. Moreover, since the constraints on the parameters are not exactly the same in both schemes, it appears in the literature that the typical values of these parameters usually differ whether the SRD CC or the SRD CFC scheme is used. We use in this study the same parameters in both kinds of SRD simulations. We detail the reasons of our choices of the parameters in the following.

#### 1. Time scale analysis

A physical system can be described at many different time scales. Some properties of a given system can be modeled assuming a clear separation of some of these time scales, while others are the consequence of a competition between phenomena that occur at time scales relatively close to each other. Two time scales of two different phenomena can be compared using dimensionless characteristic numbers that are the ratio of these time scales. The SRD fluid is a model of a fluid for which the differences between time scales can be tuned by changing the parameters. The choices of the parameters have to be made in order to (i) keep characteristic numbers in the right regimes and (ii) keep all the time scales sufficiently close to each other in order to gain computational efficiency. For example, if the real system has a Reynolds number of $10^{-6}$, a value of 0.05 is sufficiently low to keep the time scale of momentum transfer in the fluid faster than diffusive transport, but this value is also sufficiently high so that treating both momentum transfer and diffusive transport in the same simulation is not too time consuming.

In the case of solutions and suspensions, several important time scale separations have to be conserved. The Schmidt number $\mathrm{Sc} = \nu/D_f$ expresses the ratio of the time scale of diffusive mass transfer over the time scale of momentum transfer in the fluid. For a gas, Sc is close to 1 and for a liquid, it is on the order of $10^2$–$10^3$. For a SRD fluid, Sc depends on the simulation parameters $\alpha$, $\gamma$, and $\lambda$. Increasing the number of fluid particles per cell $\gamma$ leads to a liquidlike behavior, while minimizing the number of fluid particles per cell $\gamma$ decreases the computational cost. We chose the set of parameters $\{\alpha = 130^\circ, \gamma = 5, \lambda = 0.1\}$, which gives $\mathrm{Sc} \sim 10$. According to the results of Ripoll *et al.* [45], this value of the Schmidt number should be high enough for our study: While Sc varied between $\mathrm{Sc}(\lambda = 0.1) \sim 10$ and $\mathrm{Sc}(\lambda = 0.02) \sim 200$, these authors did not observe differences between the dependences on volume fraction of the diffusion coefficients of solutes computed from the SRD CC scheme. In the SRD CFC scheme, the influence of the Schmidt number is less important [24].

Another very important characteristic number is the ratio $\tau_s/\tau^\star$ between the solute velocity relaxation time $\tau_s$ and the solute diffusion time $\tau^\star$. Here $\tau^\star = \sigma_{cc}^2/4D^\circ$ is the characteristic time needed for a solute to diffuse on a length equal to its radius with a diffusion coefficient $D^\circ$. The relaxation time of the solute velocity $\tau_s$ is the characteristic time scale it takes a solute particle to reach its stationary velocity under the influence of an external force; it can be expressed as $D^\circ M/k_B T$, where $M$ is the mass of the solute. The overdamped equation of motion of BD simulations is justified only for systems for which the ratio $\tau_s/\tau^\star$ is small, which is usually the case for solutions and suspensions of relatively small solutes. In the hybrid MD-SRD schemes, the value of $D^\circ$, and therefore the ratio $\tau_s/\tau^\star$, depends on the collision scheme and must be kept small in order to compare the results with BD for times larger than $\tau_s$. It is noteworthy that $D^\circ$ is an input parameter in BD simulations, whereas it has to be computed *a posteriori* in SRD. We discuss in more detail in the following section the choice of parameters for both MD-SRD schemes and the method used to compute the value of $D^\circ$.

#### 2. Choice of solute mass in the collision coupling scheme

In the SRD CC scheme, the only parameter that controls the solute-fluid coupling is the solute's mass $M$. Ripoll *et al.* [45] performed a careful analysis of the influence of the solute's mass on the diffusion coefficient for a single solute in solution. A small value of $M$ decreases the coupling between solvent and solute and a high value increases the computation time because the displacements in MD are slower for heavy particles. What matters in our case is the evolution of the transport coefficients of solutes with the volume fraction. We have computed the self-diffusion coefficient of neutral solutes for several volume fractions with the SRD CC scheme and we have repeated this

calculation for several values of $M$ ($M = 20m_f, 10m_f, 5m_f$). We observed that the mass of the solute does not influence the dependence of the diffusion coefficient on the volume fraction within the range $[5m_f, 20m_f]$ (results not shown). In the SRD CFC scheme, the solute's mass influence is very weak. We have kept $M = 10m_f$ in the rest of the paper.

Using this value of $M$, we have computed the value of the diffusion coefficient of solutes at infinite dilution $D^\circ$. We have simply switched off the interactions between the solutes and computed the diffusion coefficient, which is then assumed to be equal to $D^\circ$. We have obtained

$$D^\circ_{\text{SRD CC}} = 4.175 \pm 0.005 \times 10^{-2} a_0^2 t_0^{-1}, \tag{14}$$

where the uncertainty is here the standard error of results obtained from several independent trajectories. From this value of $D^\circ$, the characteristic times $\tau_s$ and $\tau^\star$ can be computed: $\tau^\star = \sigma_{cc}^2/4D^\circ = 135t_0$ and $\tau_s = D^\circ M/k_B T = 0.4175t_0$. The ratio $\tau_s/\tau^\star$ is thus equal to $3 \times 10^{-3}$.

#### 3. *Choice of the fluid-solute interaction parameter in the central force coupling scheme*

In the SRD CFC scheme, the solute mass has a negligible effect on the dynamics of solutes for time scales much larger than the velocity relaxation time scale $\tau_s$. The relevant parameter characterizing the fluid-solute coupling is the interaction parameter $\sigma_{cf}$ involved in Eq. (6). Several factors must be taken into account when choosing the value of $\sigma_{cf}$ relative to $\sigma_{cc}$ and to $a_0$.

First, the value of $\sigma_{cf}$ related to the size $a_0$ of collision cells controls the accuracy of the velocity field of the fluid around the solute: The hydrodynamics at the scale of the collision cell is not properly described, so the solute size must exceed $a_0$. Padding and Louis [24] suggested the choice $\sigma_{cf} = 2a_0$. Second, the size of the simulation box has to be sufficiently large in order that the long-range hydrodynamic interactions between solutes are taken into account. However, the larger the simulation box, the longer the computation time, so a compromise must be found. We took $L_{box} > 16\sigma_{cf}$ in every case. Third, the value of $\sigma_{cf}$ compared to $\sigma_{cc}$ influences the possible depletion effect induced by fluid particles between solutes because of their finite size. It is known in hard-sphere systems that for a minimal distance of approach between two solutes less than $2\sigma_{cf}$, the depletion effect arises. Taking $\sigma_{cc} \geqslant 2\sigma_{cf}$ would then avoid depletion. When soft interaction potentials are used, in the presence of attractive interactions, as in our case due to electrostatic interactions, the minimal distance of approach between solutes $d_{min}$ is smaller than $\sigma_{cc}$. We have thus tuned $\sigma_{cc}$ until $d_{min} > 2\sigma_{cf}$ between solutes of opposite charges where interactions are attractive. Here $d_{min}$ is chosen as the largest distance for which the solute-solute radial distribution function is equal to zero (plots of the radial distribution functions can be found in Sec. IV). Finally, we have taken $\sigma_{cc} = 4.75a_0$ with $d_{min} = 4.30a_0$ for $\sigma_{cf} = 2a_0$. These parameters are the same in the SRD CC and SRD CFC coupling schemes.

We have computed the value of $D^\circ$ in the SRD CFC scheme as an extrapolation to infinite simulation box size of the self-diffusion coefficient of a unique neutral solute in solution, applying a finite-size scaling. We obtained

$$D^\circ_{\text{SRD CFC}} = 1.328 \pm 0.002 \times 10^{-2} a_0^2 t_0^{-1}, \tag{15}$$

where the uncertainty is deduced from the correlation coefficient of the linear regression of the data. The characteristic times $\tau_s$ and $\tau^\star$ are then $\tau^\star = \sigma_{cc}^2/4D^\circ = 425t_0$ and $\tau_s = D^\circ M/k_B T = 0.133t_0$. The ratio $\tau_s/\tau^\star$ is equal to $3 \times 10^{-4}$.

Using both SRD CC and SRD CFC, the ratio $\tau_s/\tau^\star$ is very small, which corresponds to the regime of overdamped dynamics. This regime is typical of most solutions and suspensions and it is the regime where Brownian dynamics is valid.

### D. Technical details

In Brownian dynamics, the time steps of simulations depend on the solute density and is between $10^{-3}\tau^\star$ and $2.5 \times 10^{-4}\tau^\star$. In every case, simulation runs without HIs of duration of the order of $100\tau^\star$ were first performed to equilibrate the systems. Ten successive trajectories of duration of about $400\tau^\star$ were computed with BD for each system. The positions and hydrodynamic velocities were saved every $4 \times 10^{-3}\tau^\star$. Then the transport coefficients were computed as averages over the ten trajectories following Eqs. (A1), (A4), and (A5) given in the Appendix.

In SRD, we took $\delta t_{MD} = 0.01t_0$ to avoid an increase of the temperature, with a time between two collisions $\delta t_c = 10\delta t_{MD}$. Each system was equilibrated for $500t_0$ and then we performed simulation runs over a duration of $5000t_0$ ($\simeq 12\tau^\star$–$40\tau^\star$ according to the coupling scheme) to produce the solute trajectories. For every system we computed the averaged transport properties from 32 independent trajectories with frames saved every four MD steps $\delta t_{frame} = 0.04t_0$. The transport coefficients were computed as averages over the ten trajectories following Eqs. (A8) and (A10).

In every case, the agreement between the self-diffusion coefficient $D^s$ obtained from mean-squared displacements or from velocity correlations was good. For systems of charged solutes, we took advantage of the symmetry between positively and negatively charged solutes in averaging the self-diffusion coefficient over all species. The package NMOLDYN [52] was used to compute correlation functions from the trajectories.

## IV. RESULTS

### A. Structure

The radial distribution functions (RDFs) between solutes obtained by SRD CFC are given in Fig. 1 for the two different systems investigated here (neutral solutes and charged solutes). In the top panel of Fig. 1, the volume fraction is the lowest one studied by SRD ($\phi = 0.033$); in the bottom panel of Fig. 1, it is the highest one ($\phi = 0.263$). The RDFs obtained from BD and SRD CC (not shown here) were exactly the same as those obtained from SRD CFC in every case, consistently with the fact that the three methods accurately sample phase space in the canonical ensemble. As can be seen in Fig. 1, the RDFs are nonzero for a distance between solutes that is the same for every system ($d_{min} = 0.95\sigma_{cc}$). The first peak between neutral solutes or solutes of opposite charges appears at distances that are only slightly larger than $\sigma_{cc}$ (between $1.08\sigma_{cc}$ and $1.16\sigma_{cc}$).

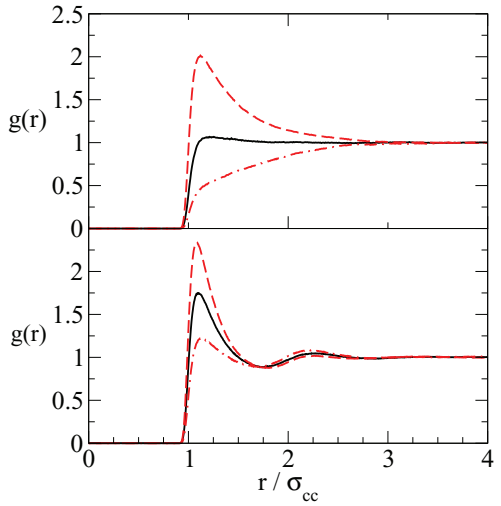


FIG. 1. (Color online) Radial distribution functions $g(r)$ between solutes for the two different systems investigated here, computed from SRD CFC simulations, for two volume fractions $\Phi$ (top, $\Phi = 0.033$; bottom, $\Phi = 0.263$). Solid black lines show RDFs between neutral solutes, dashed red lines show RDFs between solutes of opposite charges, and dot-dashed red lines show RDFs between solutes of the same charge. The same quantities were calculated with BD and with SRD CC, giving the same curves within simulation errors.

We have thus two different systems made of solutes of the same size, either neutral or charged.

### B. Self-diffusion

The self-diffusion coefficients obtained from BD and SRD schemes as functions of the solute volume fraction are plotted in Fig. 2 for the system of neutral solutes and in Fig. 3 for the system of charged solutes. The self-diffusion coefficient computed from the trajectories is here divided by the value at infinite dilution $D^\circ$, which is an input parameter in BD, and was deduced from specific computations in the SRD

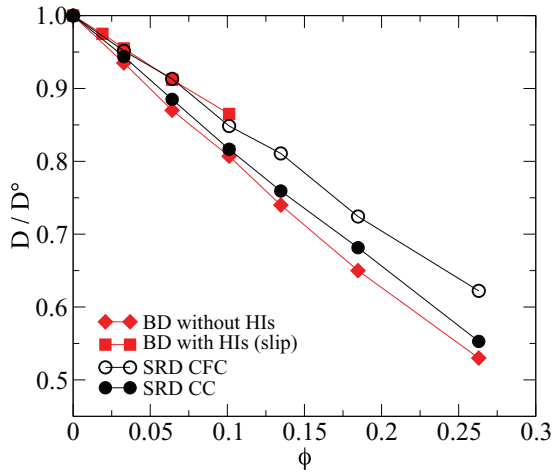


FIG. 2. (Color online) Self-diffusion coefficient of solutes divided by the value at infinite dilution as a function of the volume fraction $\Phi$ in the case of neutral solutes, for the four simulation methods (lines are guide for the eyes). In each case, the size of the symbol is much larger than the estimated statistical uncertainty of the result.

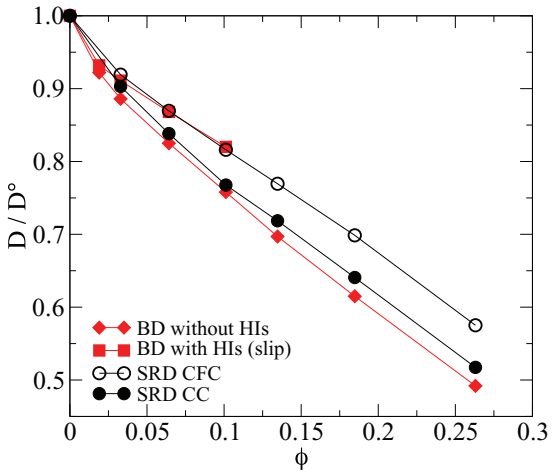


FIG. 3. (Color online) Self-diffusion coefficient of solutes divided by the value at infinite dilution as a function of the volume fraction $\Phi$ in the case of charged solutes, for the four simulation methods. Lines are guide for the eyes. In each case, the size of the symbol is much larger than the estimated statistical uncertainty of the result.

schemes [values given by Eqs. (15) and (14)]. The size of the symbols used in Figs. 2 and 3 is in every case much larger than the estimated statistical uncertainty of the result. We have computed this uncertainty as the standard error of the results obtained from several independent trajectories (10 runs in BD and 32 runs in SRD). It should be noticed that the largest value of this uncertainty is $0.001D^\circ$ in BD and $0.01D^\circ$ in SRD.

As expected, the self-diffusion coefficient as a function of the volume fraction decreases under the influence of solute-solute interactions. This decrease is more pronounced when electrostatic interactions are present. Whatever the method used to account for hydrodynamic interactions, it leads to a systematic increase of the self-diffusion coefficient compared to the case without HIs. Hydrodynamics reduces the impact of direct solute-solute interactions on long-time self-diffusion for non-hard-sphere systems, especially when strong and long-range particle repulsions exist like in charged systems [53]. Such a behavior was already observed in various systems from mode coupling theories [54–56], numerical simulations [3,57–59], and experiments [60,61]. The magnitude of the effect of hydrodynamics on self-diffusion depends on the simulation algorithm used: It is quite small in any case, but significantly larger than the uncertainty of the numerical results. For a given method, the HIs have almost the same effect on $(D^\circ - D)/D^\circ$ for all volume fractions tested. The SRD algorithm with the collision coupling scheme (SRD CC) differs only by about 2% from BD without HIs. It seems from our simulations that this method does predict only a very small effect of hydrodynamics on diffusion. The two other algorithms that account for HIs, namely, BD and SRD CFC, provide results that are very close to each other. They differ from the case of BD without HIs with a relative difference between 5% and 8%. This order of magnitude of the enhancement of the self-diffusion under the influence of hydrodynamic interactions corresponds to that already observed in other studies. This excellent agreement between BD with HIs and SRD CFC is consistent with the statement that the SRD CFC actually mimics slip boundary

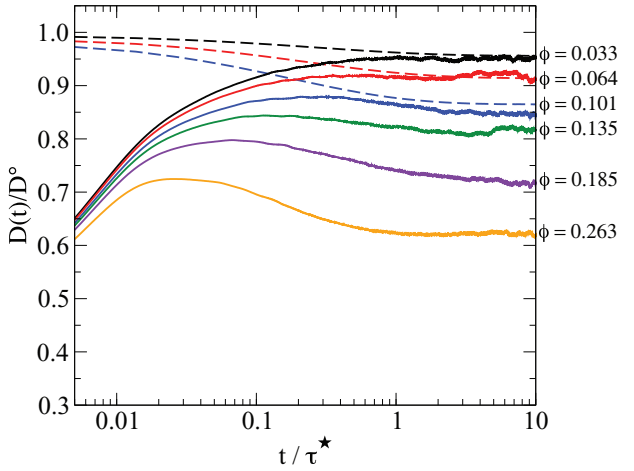


FIG. 4. (Color online) Self-diffusion coefficient of neutral solutes as a function of time obtained from BD with HIs and slip boundary conditions (A3) (dashed lines) and from SRD CFC (A9) (solid lines), for volume fractions between 0.033 and 0.263 (the volume fractions are exactly the same as those reported in Fig. 2).

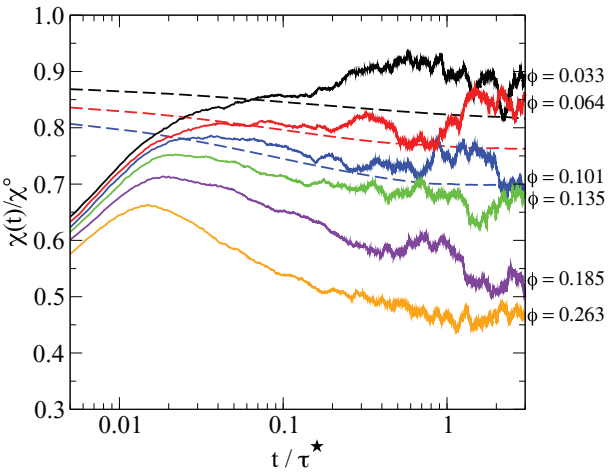


FIG. 5. (Color online) Electrical conductivity of the solution of charged solutes as a function of time divided by the value at infinite dilution $\chi^\circ$ obtained from BD with HIs and slip boundary conditions (A6) (dashed lines) and from SRD CFC (A11) (solid lines) for volume fractions between 0.033 and 0.263 (the volume fractions are exactly the same as those reported in Fig. 6).

conditions and shows that the approximate treatment of HIs in BD is sufficient to account for their main effect in the dilute range. The nonphysical position of the hydrodynamic boundary inside the solute in SRD CFC (to avoid depletion) does not seem to have a significant influence on the magnitude of hydrodynamic interactions between solutes.

Moreover, we plotted in Fig. 4 the self-diffusion coefficients of solutes as functions of time obtained from the integral of the velocity autocorrelation function with SRD CFC and the analogous function obtained with BD with slip HIs. As expected, the short-time behavior is very different in both methods: Brownian dynamics relies on an overdamped equation of motion, while the SRD CFC scheme accounts for the short-time relaxation of the velocity of solutes. Indeed, we do not expect agreement between SRD CFC and BD results at a time scale lower than the velocity relaxation time scale $\tau_s$, which is much smaller than $\tau^\star$ ($\tau_s/\tau^\star = 3 \times 10^{-4}$). In contrast, for time scales similar to (or larger than) the diffusion time $\tau^\star$, diffusion behaviors predicted by BD and SRD can be compared. We see in Fig. 4 that we do have similar long-time behaviors of the time-dependent self-diffusion coefficients computed from BD with slip HIs and with SRD CFC (time scales larger than $\tau^\star$).

### C. Electrical conductivity

We have also investigated the behavior of a collective dynamic quantity, for which hydrodynamic interactions may play a significant role, namely, the electrical conductivity of the system. It is well known that hydrodynamic couplings between solutes tend to decrease the electrical conductivity: Solutes of opposite charges travel in opposite directions under an electric field, so they drag the solvent in opposite directions. Such a result can also be obtained in simulations of charged solutions without external field, using Kubo formulas [3]. Nevertheless, it should be noted that the computation of the electrical conductivity is more affected by noise than that of the self-diffusion coefficient because it involves the integral of a collective quantity (the current of charges). The equations used to compute the electrical conductivity from BD and SRD simulations are given in the Appendix.

We show in Fig. 5 the electrical conductivity as a function of time deduced from the integrals of the autocorrelation function of the current of charges, obtained both with BD with HIs and slip boundary conditions [see Eq. (A6)] and with SRD CFC [see Eq. (A11)]. As can be seen in this figure, the noise is important for results obtained from SRD CFC because the total length of the simulations is smaller than in BD. Nevertheless, we see that for times larger than $\tau_s$ and of the order of $\tau^\star$, we obtain similar trends from BD and SRD CFC.

Since our goal is to compare several simulation techniques, we compare in what follows the values of the electrical conductivity obtained from several methods at a given time. We chose a time that is smaller than the time scale for which the integral of the autocorrelation function of the current of charges reaches a plateau, but much larger than the velocity relaxation time $\tau_s$, so it makes sense to compare SRD and BD. The values of the electrical conductivity of the systems containing charged solutes are plotted in Fig. 6 at a time close to the characteristic diffusion time: $t = 0.25\tau^\star$.

We observe in Fig. 6 that, as expected, the influence of hydrodynamics on the conductivity is more pronounced than on self-diffusion: For example, BD with HIs differs from BD without HIs by roughly 15% or so. This order of magnitude of the decrease of the conductivity induced by hydrodynamics is the same as in aqueous solutions of strong electrolytes, computed from analytical calculations [62] or numerical simulations [3] in agreement with the experimental data.

As for the comparison between SRD-based schemes and BD, part of the trends we observed for the diffusion behavior are still clearly observed for the conductivity and some of them are amplified. The electrical conductivity obtained with SRD CC is closer to the value obtained with BD without HIs than the conductivity obtained with SRD CFC. Nevertheless, we

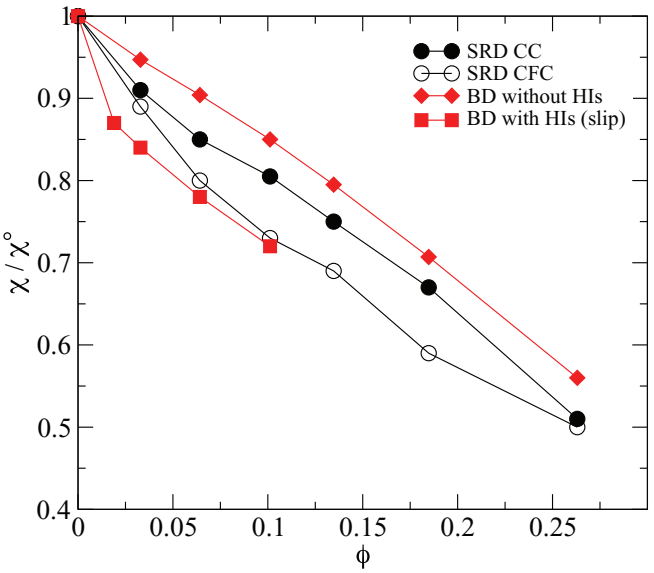


FIG. 6. (Color online) Electrical conductivity of the solution divided by the value at infinite dilution as a function of the volume fraction $\Phi$ in the case of charged solutes obtained from the four simulation methods at $t = 0.25\tau^\star$.

obtain a significant and systematic difference between SRD CC and BD without HIs (difference of about 6%), contrarily to what was observed for self-diffusion (difference between both $D/D^\circ$ values smaller than 2%). This means that there is a non-negligible and systematic effect of the hydrodynamic couplings between solutes when the solute is coupled to the solvent through the SRD CC scheme, even if for our systems these couplings do not influence the self-diffusion behavior very much. As in the case of self-diffusion, the electrical conductivity computed with the SRD CFC scheme is close to that computed with BD with slip boundary conditions. The agreement between both methods is not as good as for self-diffusion (the difference between SRD CFC and BD with slip HIs for $D/D^\circ$ was on the order of 2%), which may be due to the relatively high level of noise in the computation of the autocorrelation function of the current in SRD CFC, which can be seen in Fig. 6.

Finally, the influence of the choice of the coupling method between solutes and fluid particles in SRD seems also amplified for the calculation of the electrical conductivity: Except for the smallest and largest values of the volume fraction, the difference between the values obtained with SRD CC and SRD CFC is of the order of 7%, compared to 3% for self-diffusion.

## V. CONCLUSION

The multiplicity of the methods available to simulate the dynamics of particles embedded in a solvent, ranging from small ions to micrometric colloidal particles, offers a difficult choice. In this article, we compared for model systems the self-diffusion coefficient and the electrical conductivity obtained by two different coupling schemes between solute and solvent in SRD (SRD CC and SRD CFC schemes), with strictly the same parameters to describe the SRD fluid. We obtained systematic differences between both SRD schemes, which are mainly due to the different treatments of the short-range fluid-solute interaction: SRD CC treats solutes as pointlike from the hydrodynamic point of view, whereas a clear boundary exists between fluid and solutes in the SRD CFC scheme. For dilute systems, with a volume fraction less that 0.1, BD with HIs also allows one to compute individual and collective transport properties. Hydrodynamic interactions can be disregarded in BD, providing reference values to quantify the hydrodynamic couplings in other methods.

We found remarkable agreement between BD and SRD when the solute interacts with the SRD fluid through direct central forces (SRD CFC) and when slip boundary conditions are taken in BD, be it for the self-diffusion coefficients of solutes or for the electrical conductivity of the solution when solutes are charged. Conversely, when solutes are coupled to the SRD fluid during the collision step (SRD CC), the effect of hydrodynamics on the self-diffusion is much less noticeable than with BD, even if a systematic effect of HIs exists on the electrical conductivity. The SRD CC is an attractive method because it is faster than SRD CFC, but our results show that it does not provide a quantitative description of the influence of hydrodynamic interactions on the diffusion of solutes at equilibrium; SRD CC better accounts for the influence of hydrodynamic couplings on the electrical conductivity, which is a collective transport property. Nevertheless, in many systems the precise hydrodynamic boundary condition is unknown, typically for polymers or polyelectrolytes. In such cases, the fact that the SRD CC method does not account for the short-range solvent-solute direct interaction that leads to stick, slip, or no-slip boundary conditions does not prevent the use of the method and since it is faster, it may be the best option.

Finally, as far as dilute bulk suspensions or solutions are concerned, our comparative study also showed that, from the point of view of the numerical efficiency, BD, because it is based on an overdamped equation of motion and assumes that the solvent is a continuous medium, is much more efficient than SRD-based simulations to compute trajectories over time scales larger than the diffusion time scale $\tau^\star$. Of course, for cases where BD fails to be reliable or cannot be used (concentrated systems and systems under flow or under confinement), the resort to SRD-based or other algorithms is mandatory.

## ACKNOWLEDGMENTS

G.M., V.D., and M.J. acknowledge financial support from the French National Agency for Research under Grant No. ANR-09-JCJC-0082-01.

## APPENDIX: COMPUTATION OF TRANSPORT COEFFICIENTS

### 1. 1. Brownian dynamics simulations

To obtain the self-diffusion coefficient of ions $D$, we calculate the autocorrelation function of the hydrodynamic velocity with a Kubo-like relation derived from a linear response theory at the Smoluchowski level [3,63]:

$$D = \frac{1}{3}\left[\langle \mathrm{tr}\{\mathbf{D}_{ii}\}\rangle - \int_0^\infty \langle \mathbf{U}_i(t_0+t)\cdot\mathbf{U}_i(t_0)\rangle_{t_0} dt\right], \qquad \text{(A1)}$$

where $\mathbf{U}_i(t_0)$ and $\mathbf{U}_i(t_0+t)$ are the hydrodynamic velocities of the particle $i$ at some arbitrary initial time $t_0$ and at some later

time $t + t_0$, respectively, the angular brackets specify averages over the particles $i$ and over the time $t_0$, and $\mathrm{tr}\{\mathbf{D}_{ii}\}$ is the trace of the diffusion submatrix $\mathbf{D}_{ii}$. The hydrodynamic velocity is defined as

$$\mathbf{U}_i(t) = \sum_{j=1}^{N} \mathbf{D}_{ij}(t) \cdot \mathbf{F}_j(t), \tag{A2}$$

with $\mathbf{F}_j(t)$ the total force acting on particle $j$ at time $t$. The self-diffusion coefficient as a function of time divided by the value at infinite dilution is thus

$$\frac{D(t)}{D^\circ} = \frac{1}{3D^\circ}\left[\langle \mathrm{tr}\{\mathbf{D}_{ii}\}\rangle - \int_0^t \langle \mathbf{U}_i(t_0 + t') \cdot \mathbf{U}_i(t_0)\rangle_{t_0} dt'\right]. \tag{A3}$$

The autocorrelation function (A1) tends to zero with a rather small characteristic time, so we were particularly careful in the sampling of small times. An alternative way to obtain the self-diffusion coefficient is to compute the slope of the mean-square displacements at long times:

$$\langle |\mathbf{r}_i(t + t_0) - \mathbf{r}_i(t_0)|^2\rangle_{t_0} = 6Dt, \tag{A4}$$

where a long-time average ($t \to \infty$) is implied.

The electrical conductivity $\chi$ of charged systems is also computed from a Kubo-like relation, which reads

$$\chi = \frac{1}{3}\frac{\beta}{V}\left(\left\langle \sum_{i=1}^{N}\sum_{j=1}^{N} q_i q_j \ \mathrm{tr}\{\mathbf{D}_{ij}\}\right\rangle - \int_0^\infty dt \left\langle \sum_{i=1}^{N} q_i \mathbf{U}_i(t_0 + t) \cdot \sum_{j=1}^{N} q_j \mathbf{U}_j(t_0)\right\rangle_{t_0}\right), \tag{A5}$$

where $q_i = Z_i e$ is the electric charge of the $i$th particle and $\beta = 1/k_B T$, so the value at a given time time $t$ is

$$\chi(t) = \frac{1}{3}\frac{\beta}{V}\left(\left\langle \sum_{i=1}^{N}\sum_{j=1}^{N} q_i q_j \ \mathrm{tr}\{\mathbf{D}_{ij}\}\right\rangle - \int_0^t dt' \left\langle \sum_{i=1}^{N} q_i \mathbf{U}_i(t_0 + t') \cdot \sum_{j=1}^{N} q_j \mathbf{U}_j(t_0)\right\rangle_{t_0}\right). \tag{A6}$$

The electrical conductivity at infinite dilution reads

$$\chi^\circ = \frac{\beta}{V}\sum_i q_i^2 N_i D_i^\circ, \tag{A7}$$

where $N_i$ is the number of charged solutes of type $i$ in the simulation box and $V$ is the volume of the simulation box.

The two Kubo-like expressions (A1) and (A5) consist of two contributions. The first one is due to the instantaneous response of the system, which can be viewed as the sum of the infinite dilution conductivity (or diffusion) and an electrophoretic correction if hydrodynamic interactions are taken into account. The second one is due to the time-dependent retarded response (still with instantaneous hydrodynamic interactions in our treatment) describing relaxation effects, including direct and hydrodynamic interactions.

### 2. Stochastic rotational dynamics simulations with embedded solutes

In SRD with embedded solutes, the self-diffusion coefficient $D$ is computed from the same functions as in molecular dynamics. The mean-square displacement formula is the same as in BD, but the equivalent Kubo relation is written

$$D = \frac{1}{3}\int_0^\infty dt \langle (\mathbf{v}_i(t_0) \cdot \mathbf{v}_i(t + t_0))\rangle_{t_0}. \tag{A8}$$

The self-diffusion coefficient with time then reads

$$\frac{D(t)}{D^\circ} = \frac{1}{3D^\circ}\int_0^t dt' \langle \mathbf{v}_i(t_0) \cdot \mathbf{v}_i(t_0 + t')\rangle_{t_0}. \tag{A9}$$

The electrical conductivity of the system reads

$$\chi = \frac{\beta}{3V}\int_0^\infty dt \left\langle \sum_i^N q_i \mathbf{v}_i(t_0) \cdot \sum_i^N q_i \mathbf{v}_i(t_0 + t)\right\rangle_{t_0}, \tag{A10}$$

so we have the conductivity as a function of time

$$\chi(t) = \frac{\beta}{3V}\int_0^t dt' \left\langle \sum_i^N q_i \mathbf{v}_i(t_0) \cdot \sum_i^N q_i \mathbf{v}_i(t_0 + t')\right\rangle_{t_0}. \tag{A11}$$

The electrical conductivity at infinite dilution $\chi^\circ$ is again given by Eq. (A7).


[1] D. L. Ermak, J. Chem. Phys. **62**, 4189 (1975).
[2] D. L. Ermak and J. A. McCammon, J. Chem. Phys. **69**, 1352 (1978).
[3] M. Jardat, O. Bernard, P. Turq, and G. R. Kneller, J. Chem. Phys. **110**, 7993 (1999).
[4] M. Jardat, S. Durand-Vidal, P. Turq, and G. R. Kneller, J. Mol. Liq. **85**, 45 (2000).
[5] T. Yamaguchi, Y. Shimoda, and S. Koda, J. Chem. Phys. **134**, 244506 (2011).
[6] D. M. Heyes, Mol. Phys. **87**, 287 (1996).
[7] E. Wajnryb, P. Szymczak, and B. Cichocki, Physica A **335**, 339 (2004).
[8] G. Mériguet, M. Jardat, and P. Turq, J. Chem. Phys. **123**, 144915 (2005).
[9] M. Rex and H. Löwen, Eur. Phys. J. E **26**, 143 (2008).
[10] M. Dlugosz, J. M. Antosiewicz, P. Zielinski, and J. Trylska, J. Phys. Chem. B **116**, 5437 (2012).
[11] S. Jäger, H. Schmidle, and S. H. L. Klapp, Phys. Rev. E **86**, 011402 (2012).
[12] B. Liu and B. Dünweg, J. Chem. Phys. **118**, 8061 (2003).
[13] N. Kikuchi, J. F. Ryder, C. M. Pooley, and J. M. Yeomans, Phys. Rev. E **71**, 061804 (2005).
[14] T. Zhou and S. B. Chen, J. Chem. Phys. **122**, 124905 (2005).
[15] R. Pamies, J. G. Hernandez Cifre, and J. Garcia De La Torre, J. Polym. Sci. B **45**, 714 (2007).
[16] C. Stoltz, J. J. de Pablo, and M. D. Graham, J. Chem. Phys. **126**, 124906 (2007).
[17] J. Rotne and S. Prager, J. Chem. Phys. **50**, 4831 (1969).

[18] B. Cichocki, R. B. Jones, R. Kutteh, and E. Wajnryb, J. Chem. Phys. **112**, 2548 (2000).
[19] J. P. Hernandez-Ortiz, J. J. de Pablo, and M. D. Graham, Phys. Rev. Lett. **98**, 140602 (2007).
[20] A. J. C. Ladd, J. Chem. Phys. **93**, 3484 (1990).
[21] A. Malevanets and R. Kapral, J. Chem. Phys. **110**, 8605 (1999).
[22] G. Gompper, T. Ihle, D. M. Kroll, and R. G. Winkler, in *Advanced Computer Simulation Approaches for Soft Matter Sciences III*, edited by C. Holm and K. Kremer (Springer, Berlin, 2009), Vol. 221, pp. 1–87.
[23] A. Malevanets and R. Kapral, J. Chem. Phys. **112**, 7260 (2000).
[24] J. T. Padding and A. A. Louis, Phys. Rev. E **74**, 031402 (2006).
[25] J. T. Padding, A. Wysocki, H. Löwen, and A. A. Louis, J. Phys.: Condens. Matter **17**, S3393 (2005).
[26] J. K. Whitmer and E. Luijten, J. Phys.: Condens. Matter **22**, 104106 (2010).
[27] I. O. Götze and G. Gompper, Phys. Rev. E **84**, 031404 (2011).
[28] S. Hanot, M. Belushkin, and G. Foffi, Soft Matter **9**, 291 (2013).
[29] S. Frank and R. G. Winkler, Europhys. Lett. **83**, 38004 (2008).
[30] S. Frank and R. G. Winkler, J. Chem. Phys. **131**, 234905 (2009).
[31] J. X. Chen and R. Kapral, J. Chem. Phys. **134**, 044503 (2011).
[32] M. Hecht, J. Harting, T. Ihle, and H. J. Herrmann, Phys. Rev. E **72**, 011408 (2005).
[33] A. Tomilov, A. Videcoq, T. Chartier, T. Ala-Nissilä, and I. Vattulainen, J. Chem. Phys. **137**, 014503 (2012).
[34] J. T. Padding and A. A. Louis, Phys. Rev. Lett. **93**, 220601 (2004).
[35] J. T. Padding and A. A. Louis, Phys. Rev. E **77**, 011402 (2008).
[36] A. Moncho-Jorda, A. A. Louis, and J. T. Padding, Phys. Rev. Lett. **104**, 068301 (2010).
[37] D. Lüsebrink and M. Ripoll, J. Chem. Phys. **137**, 194904 (2012).
[38] J. Sané, J. T. Padding, and A. A. Louis, Phys. Rev. E **79**, 051402 (2009).
[39] B. Dünweg and A. J. C. Ladd, in *Advanced Computer Simulation Approaches for Soft Matter Sciences III* (Ref. [22]), pp. 89–166.
[40] V. Dahirel, M. Jardat, J.-F. Dufrêche, and P. Turq, J. Chem. Phys. **126**, 114108 (2007).
[41] V. Dahirel, B. Ancian, M. Jardat, G. Mériguet, P. Turq, and O. Lequin, Soft Matter **6**, 517 (2010).
[42] M. Jardat, T. Cartailler, and P. Turq, J. Chem. Phys. **115**, 1066 (2001).
[43] T. Ihle and D. M. Kroll, Phys. Rev. E **63**, 020201(R) (2001).
[44] T. Ihle and D. M. Kroll, Phys. Rev. E **67**, 066705 (2003).
[45] M. Ripoll, K. Mussawisade, R. G. Winkler, and G. Gompper, Phys. Rev. E **72**, 016701 (2005).
[46] N. G. Van Kampen, *Stochastic Processes in Physics and Chemistry* (North-Holland, Amsterdam, 1987).
[47] P. J. Rossky, J. D. Doll, and H. L. Friedman, J. Chem. Phys. **69**, 4628 (1978).
[48] D. M. Heyes and A. C. Brańka, Mol. Phys. **94**, 447 (1998).
[49] D. M. Heyes and A. C. Brańka, Mol. Phys. **98**, 1949 (2000).
[50] B. U. Felderhof, Physica A **89**, 373 (1977).
[51] E. Falck, J. M. Lahtinen, I. Vattulainen, and T. Ala-Nissilä, Eur. Phys. J. E **13**, 267 (2004).
[52] T. Róg, K. Murzyn, K. Hinsen, and G. R. Kneller, J. Comput. Chem. **24**, 657 (2003).
[53] G. Nägele, J. K. G. Dhont, and G. Meier, in *Diffusion in Condensed Matter*, edited by P. Heitjans and J. Kärger (Springer, Berlin, 2005), pp. 620–715.
[54] G. Nägele and P. Baur, Physica A **245**, 297 (1997).
[55] G. Nägele and P. Baur, Europhys. Lett. **38**, 557 (1997).
[56] J.-F. Dufrêche, M. Jardat, P. Turq, and B. Bagchi, J. Phys. Chem. B **112**, 10264 (2008).
[57] R. Pesché and G. Nägele, Phys. Rev. E **62**, 5432 (2000).
[58] R. Pesché, M. Kollmann, and G. Nägele, J. Chem. Phys. **114**, 8701 (2001).
[59] M. Jardat, S. Durand-Vidal, N. da Mota, and P. Turq, J. Chem. Phys. **120**, 6268 (2004).
[60] K. Zahn, J. M. Méndez-Alcaraz, and G. Maret, Phys. Rev. Lett. **79**, 175 (1997).
[61] W. Härtl, J. Wagner, Ch. Beck, F. Gierschner, and R. Hempelmann, J. Phys.: Condens. Matter **12**, A287 (2000).
[62] J.-F. Dufrêche, O. Bernard, S. Durand-Vidal, and P. Turq, J. Phys. Chem. B **109**, 9873 (2005).
[63] B. U. Felderhof and R. B. Jones, Physica A **119**, 591 (1983).